

Just Shift It: Test-Time Prototype Shifting for Zero-Shot Generalization with Vision-Language Models

Elaine Sui, Xiaohan Wang, and Serena Yeung-Levy

Stanford University
{esui, xhanwang, syeung}@stanford.edu

Abstract. Advancements in vision-language models (VLMs) have propelled the field of computer vision, particularly in the zero-shot learning setting. Despite their promise, the effectiveness of these models often diminishes due to domain shifts in test environments. To address this, we introduce the **Test-Time Prototype Shifting (TPS)** framework, a pioneering approach designed to adapt VLMs to test datasets using unlabeled test inputs. Our method is based on the notion of modulating per-class prototypes in the shared embedding space. By pre-computing and caching prototypes generated with the pre-trained text encoder, TPS not only facilitates optimization-free prototype reuse for subsequent predictions but also enables seamless integration with current advancements in prompt engineering. At test-time, TPS dynamically learns shift vectors for each prototype based solely on the given test sample, effectively bridging the domain gap and enhancing classification accuracy. A notable aspect of our framework is its significantly reduced memory and computational demands when compared to conventional text-prompt tuning methods. Extensive evaluations across 15 datasets involving natural distribution shifts and cross-dataset generalization demonstrate TPS’s superior performance, achieving state-of-the-art results while reducing resource requirements. Code is available at <https://github.com/elaine-sui/TPS>.

Keywords: test-time adaptation · vision-language models · zero-shot

1 Introduction

In recent years, the field of computer vision has witnessed remarkable progress, largely fueled by the emergence of robust vision-language foundation models [9, 38]. These models, upon undergoing pre-training on large-scale datasets, acquire a deep understanding of visual concepts, enabling their seamless application to a range of downstream tasks without task-specific training. While these foundation models exhibit much better zero-shot generalization abilities compared to ImageNet pre-trained models, they still suffer from performance degradation due to domain shifts at test-time.

To address this problem, prior studies have explored various fine-tuning techniques, ranging from traditional full-model tuning to more parameter-efficient

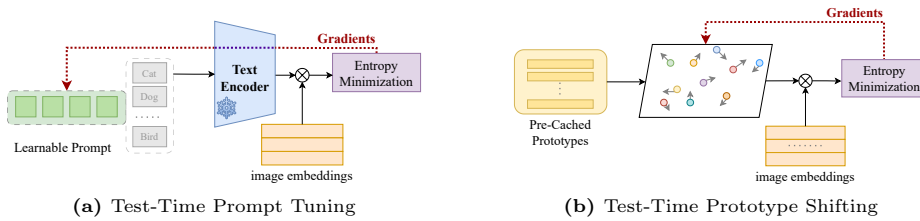


Fig. 1: Comparison of Test-Time Prompt Tuning (TPT) [43] against our method, Test-Time Prototype Shifting (TPS). TPT requires gradients to backpropagate through the large text encoder in order to reach the tuneable prompt, incurring high memory and computational costs. In contrast, TPS only backpropagates gradients to the feature space, in which our class prototype shifts are learned, making it much more efficient.

methods such as tuning additional adapters [8, 16] or input prompts [20, 22]. Nevertheless, these strategies necessitate having enough labeled data for effective fine-tuning, posing challenges in domains where acquiring labeled data is difficult. In light of this, we turn our attention to the emerging paradigm of test-time adaptation (TTA), where model parameters are adjusted in an unsupervised manner with unlabeled test inputs.

How can we effectively enable test-time adaptation using these advanced vision-language models (VLMs)? There have been relatively few initiatives in this area. A notable example is the Test-Time Prompt Tuning (TPT) method [43], which suggests fine-tuning several prompt tokens of the text input for each individual unlabeled test sample. However, this approach faces practical constraints due to the significant memory and computational demands involved in back-propagating through the text encoder for each image.

In this work, we propose **Test-Time Prototype Shifting (TPS)**, a simple yet effective framework that specifically adjusts per-class prototypes within the embedding space. Initially, we compute each class prototype using the pre-trained text encoder from a VLM, enabling the prototypes to be cached and reused for all subsequent predictions. At test-time, we adapt by learning a shift vector for each prototype on the fly for a single test sample, bridging the domain gap between the prototypes and the target sample. A key highlight of our framework is that the shift vectors are the only parameters being updated and are adjusted within the embedding space itself, circumventing the need for back-propagation through the text and visual encoders. In comparison to TPT, our TPS framework achieves a **10 times** increase in speed while necessitating less than **1/10** of the memory cost.

Benefiting from the two-stage learning paradigm, our approach fully capitalizes on the advancements in prompt engineering. Prototypes can be generated using vanilla templates such as “*a photo of a {class}.*”, or crafted using more sophisticated, well-designed prompts [30, 38, 52] that significantly enhance generalization capabilities. Furthermore, experiments with few-shot learning on ImageNet reveal that learnable prompts are highly effective in addressing natural domain shifts [56, 57]. In our study, we build upon these previous advancements

by generating improved prototypes that can be seamlessly integrated into our Test-Time Prototype Shifting framework.

The zero-shot generalization capabilities of TPS were extensively evaluated across two distinct series of datasets: those involving natural distribution shifts and those focused on cross-dataset generalization. Our TPS consistently outperforms CLIP baselines, and surpasses current state-of-the-art (SoTA) by **3.3%** on the natural distribution shifts benchmark and **1.9%** on the cross-dataset generalization benchmark, respectively. Moreover, we demonstrate that regardless of the prototype-generation approach, learning a feature-space shift on the prototypes consistently boosts performance over zero-shot CLIP by over **4%** on natural distribution shifts and up to **1%** on cross-dataset generalization benchmarks. Remarkably, our approach not only outperformed TPT in terms of top-1 accuracy but also achieved this with only **1/10** of the memory and time costs.

Our main contributions are summarized as follows:

1. We introduce the Test-time Prototype Shifting (TPS) framework, a novel, straightforward and efficient approach. This is, to our knowledge, the first instance of utilizing feature space modulation for test-time adaptation with VLMs.
2. Our TPS framework is designed to seamlessly integrate with existing advancements in prompt engineering, transforming it into a flexible plug-and-play system.
3. We achieve state-of-the-art performance on both natural distribution shift and cross-dataset generalization benchmarks, surpassing current SoTA by 3.3% and 1.9%, respectively. Additionally, our approach significantly reduces computational and memory demands by more than 10 times compared to TPT.

2 Related Works

2.1 Test-Time Adaptation

Test-time adaptation (TTA) is the task of adapting a model’s weights on an unlabeled out-of-distribution test set in order to achieve higher test performance. In the context of vision tasks, traditional methods leverage ImageNet-pretrained image classifiers and use techniques such as computing pseudo-prototype class representations to update the linear classifier [18], learning better feature representations through self-supervised auxiliary tasks [24, 26, 46], adapting the normalization layers to learn the statistics of the target distribution [32, 33, 41, 44, 49], as well as minimizing prediction entropy to increase the confidence of predictions [10, 32, 33, 49, 53]. With the development of CLIP [38], recent work in TTA has been predominantly based on prompt tuning. This involves learning a tuneable text and/or image prompt to encode the visual distribution shift while maintaining the strong performances of these foundation models by keeping the pre-trained parameters fixed [7, 12, 28, 43, 55]. Despite only tuning a relatively

small number of prompt parameters, tuning the input requires backpropagating through their respective encoders, which is especially memory intensive with large input sizes, making it infeasible in practice. Recently, an image diffusion-based method DiffusionTTA [37] has been proposed for TTA, involving updating classifier weights by training for the auxiliary task of image reconstruction using a conditional diffusion model. Nevertheless, this also necessitates backpropagation through the classifier and diffusion model. In contrast, this work proposes to avoid backpropagation through the encoders and maintain the richness of the CLIP embedding space by directly modulating the features within it.

Current TTA methods also comprise those that are considered training-free [11, 47]. Approaches include adding a parameter-free attention module to modulate multi-modal features [11] and computing the similarity between the target image and those from a constructed support set [47]. Although our work does not directly fit this setting, we follow the same spirit of minimally adjusting intermediate representations to close the domain gap.

2.2 Feature Modulation

Feature modulation is a parameter-efficient tuning paradigm where features are perturbed to better conform to a target task. This learned perturbation is typically in the form of feature normalization, achieved by modulating the encoder’s normalization layers to align source and target tasks [3, 17, 19, 36, 48]. However, modulation can also be applied more directly to the features themselves [23, 58]. For example, SSF [23] proposes to learn scale and shift parameters for each layer’s activations. DN [58] proposes to subtract the means of the text and image embeddings from the respective inputs before computing CLIP similarity to align the CLIP training and inference procedures. We propose a more simplistic feature modulation procedure where we only learn shift vectors to pre-computed class prototypes in test-time training to better align them with the out-of-distribution image embeddings of the target dataset.

2.3 Prompting for Vision-Language Models

Vision-language models enable zero-shot generalization to downstream datasets via prompting. As predictions are computed by cosine similarity of the text and image embeddings, the quality of the text embeddings or class prototypes can cause a drastic difference in performance. In the case of image classification, this entails the careful design of natural language text descriptions for each of the class names, focusing on the visual aspects apparent from the image itself [38]. CoOp [56] removes the need for hand-crafting prompts by prompt-tuning in the few-shot setting and CoCoOp [57] extends CoOp by learning instance-conditioned prompts, improving generalization ability. Another paradigm of prompt-engineering includes prompting large language models (LLMs) for better prompt templates [25] and/or content [30, 52]. Specifically, Menon and Vondrick [30] and Yang *et al.* [52] both prompt GPT-3 [2] to generate concepts or descriptors of class names to increase zero-shot and linear-probe performance on

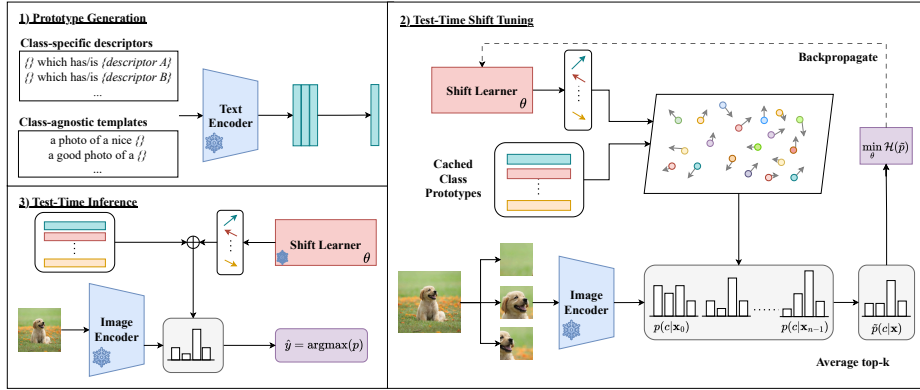


Fig. 2: We illustrate the three stages of **Test-Time Prototype Shifting (TPS)**. **1) Prototype Generation:** pre-computation of class prototypes using different prompt-engineering strategies. We show the computation of k class-conditioned descriptors for a single class. Means are computed and cached. **2) Test-Time Shift Tuning:** one iteration of test-time training where we tune the Shift Learner to generate small perturbations to the class prototypes to close the gap between the source and target distributions. Marginal entropy of the CLIP similarities of the shifted prototypes and augmented image embeddings is minimized. **3) Test-Time Inference:** Using the tuned Shift Learner, we compute the final prediction for the shifted class prototypes and the original image embedding with CLIP similarity.

image classification while providing model interpretability. Our work leverages these developments in prompt-engineering in our prototype generation phase, using these techniques to generate more knowledge-rich prototypes that can be swapped into the framework in a plug-and-play manner.

3 Method

3.1 Background

Test-Time Adaptation. Let f_{θ} be a model trained on data from some source distribution and \mathcal{D}_{test} be some unlabeled out-of-distribution test dataset. Then, the goal of test-time adaptation is to adapt θ such that the performance of f_{θ} on \mathcal{D}_{test} increases without the use of ground-truth test labels. Following [43, 54], we consider the single-input TTA setting where f_{θ} is adapted independently for every test example $d \in \mathcal{D}_{test}$.

Image Classification with CLIP. CLIP [38] is a large-scale vision-language model pre-trained by contrasting millions of (image, text) pairs. It consists of a text encoder $f_{\mathcal{T}}$ and an image encoder $f_{\mathcal{V}}$. To classify an image v with CLIP, we use the CLIP pre-trained image encoder $f_{\mathcal{V}}$ to obtain a visual feature representation $\mathbf{x} = f_{\mathcal{V}}(v)$. Then, each label in the target label set $c \in \mathcal{C}_{target}$ is transformed with prompt template \mathbf{p} . Each prompt is embedded with the pre-trained text

encoder $f_{\mathcal{T}}$ to produce prototypes $\mathbf{p}_c = f_{\mathcal{T}}(\mathbf{p}(c))$. The cosine similarities are computed between all class prototypes $\{\mathbf{p}_c\}_{c \in \mathcal{C}}$ and the visual embedding $\{\mathbf{x}\}$ to get a probability distribution over all classes.

3.2 Test-Time Prototype Shifting

Our method comprises three stages: Prototype Generation, Test-Time Shift Tuning, and Test-Time Inference, as depicted in Figure 2. Initially, in the Prototype Generation stage, we simply compute the class prototypes by embedding each class template $c \in \mathcal{C}$ of the test dataset. The vanilla prompt is “*a photo of a {class}.*”, with more advanced techniques discussed in Section 3.2.2. In the Test-Time Shift Tuning stage, shift vectors are generated through the Shift Learner to modify the prototypes (Section 3.2.1), and cosine similarities between augmented image embeddings and shifted class prototypes are used to produce n probability distributions. We optimize the Shift Learner to minimize the entropy of the aggregated marginal distribution. Finally, in the Test-Time Inference stage (Section 3.2.3), we predict the class by comparing the cosine similarities between the learned shifted text embeddings and the original image embedding, choosing the class with the highest probability.

3.2.1 Feature-Space Shift

The Test-Time Prompt Tuning (TPT) method, as proposed by Shu *et al.* [43], necessitates backpropagation through the text encoder at every test-time training step to learn the text prompt vectors. This process results in substantial computational and memory demands, which significantly hinders its practical applicability. Essentially, prompt tuning, when used for test-time adaptation, acts as an indirect technique for adjusting text embeddings. Its primary goal is to bridge the domain gap, simultaneously leveraging the multi-modal embedded knowledge of CLIP. Such considerations bring us to a pivotal question: why not directly modulate class prototypes within the embedding space? This has inspired the development of our Shift Learner module, designed specifically for learning modifications to the text embeddings. This approach not only capitalizes on the exceptional quality of the CLIP representation space but also adeptly avoids the requirement for the computationally demanding gradient backpropagation through the text encoder.

Rather than indirectly altering embeddings through prompt tuning, our approach is to directly learn to shift class prototypes within the embedding space. This strategy enables us to preserve the overarching architecture of the CLIP embedding space, while adjusting the class prototypes for better alignment with out-of-distribution visual embeddings. Our key proposition involves learning shifts for specific class prototypes, as opposed to a universal shift applicable to all classes. We recognize that domain gaps often consist of both dataset-level shifts (for example, transitioning from natural images to sketches) and class-level distribution shifts (such as differences between indoor and outdoor settings for dogs). A universally applied prototype shift, although effective for dataset-level

adjustments, lacks the nuanced expressiveness required for class-level corrections. This is because it alters each prototype identically, maintaining the relative distances between class prototypes even after test-time training.

On the contrary, class-specific shifts have the capability to accommodate both levels of distribution shifts, enhancing their generalizability across various target datasets. Although adopting class-specific shifts results in the number of tunable parameters increasing linearly with the number of classes, this added complexity is minimal compared to the computational requirements of computing and storing gradients for the sizable text encoder.

We formally elaborate on the operation of our per-class shift as follows, given class $c \in \mathcal{C}$ and corresponding class prototype $\mathbf{p}_c \in \mathbb{R}^d$, we learn a shift vector $\mathbf{s}_c \in \mathbb{R}^d$. The shift operation is performed by channel-wise addition between the class prototype \mathbf{p}_c and the learned shift vector \mathbf{s}_c . The normalized shifted prototype $\mathbf{p}'_c \in \mathbb{R}^d$ is generated as follows,

$$\mathbf{p}'_c = \frac{\mathbf{p}_c + \mathbf{s}_c}{\|\mathbf{p}_c + \mathbf{s}_c\|_2} \quad (1)$$

3.2.2 Advanced Prototype Generation

While it is effective to enhance the zero-shot generalization capabilities of vision-language models (VLMs) through test-time training, another line of techniques focuses on crafting sophisticated prompts to elevate performance. Our Test-Time Prototype Shifting framework is uniquely positioned in this landscape. By learning shifts on pre-computed and cached class prototypes, TPS is designed to be seamlessly compatible with any existing prompt-engineering methods. This integration empowers the generation of more robust and effective prototypes, leveraging advanced prompting strategies and offline prototype adjustment.

In our research, we concentrate on unsupervised test-time adaptation. Consequently, we operate under the assumption that test images are unavailable before they are individually encountered at test-time, and specific knowledge about the type of domain shift is absent. For fair comparisons, we refrain from using target-domain-specific prompts. For instance, we avoid employing prompts such as “*a photo of a sketch {class}*” exclusively for ImageNet Sketch, as this would imply prior knowledge of the domain shift type, which is contrary to our testing conditions. In this work, we employ three distinct prompt techniques: class-agnostic prompts using the set of 80 hand-crafted templates provided by CLIP [38] for ImageNet, class-specific prompts derived from intricate class descriptions generated by GPT-4 [34], and learnable prompts such as CoOp [56] and CoCoOp [57].

Aggregating class-specific representations. Our framework requires a single representation per class, but if such a representation is derived from a single prompt, the amount of information that it carries is limited to the number of input tokens that the CLIP text encoder was trained with. Hence, it would be

Algorithm 1 Test-Time Prototype Shifting (TPS)

Require: pre-trained and frozen image encoder f_V from a VLM, pre-computed class prototypes \mathbf{p}_c and trainable shift parameters \mathbf{s}_c for $c \in \mathcal{C}$, test image v_0 , set of augmentations \mathcal{A} , number of augmentations $(n - 1)$

- 1:
- 2: **function** TRAIN($v_0, \mathcal{A}, f_V, \{\mathbf{p}_c\}_{c \in \mathcal{C}}, \{\mathbf{s}_c\}_{c \in \mathcal{C}}$)
- 3: Sample $a_1, \dots, a_{n-1} \in \mathcal{U}(\mathcal{A})$
- 4: $v_i = a_i(v_0)$, $\mathbf{x}_i = f_V(v_i)$ for $i \in \{0, \dots, n - 1\}$
- 5: $\mathbf{p}'_c = (\mathbf{p}_c + \mathbf{s}_c) / \|\mathbf{p}_c + \mathbf{s}_c\|_2$ for $c \in \mathcal{C}$
- 6: Compute $p(c|\mathbf{x}_i, \mathbf{p}'_c)$ by Eq 2
- 7: Compute $\tilde{p} = \frac{1}{k} \sum_{i=1}^k p(c|\mathbf{x}'_i, \mathbf{p}'_c)$ for \mathbf{x}'_i in top- k
- 8: Compute \mathcal{L} by Eq 3
- 9: Compute $\partial \mathcal{L}$
- 10: Update $\{\mathbf{s}_c\}_{c \in \mathcal{C}}$
- 11: **end function**
- 12:
- 13: **function** TEST($v_0, f_V, \{\mathbf{p}_c\}_{c \in \mathcal{C}}, \{\mathbf{s}_c\}_{c \in \mathcal{C}}$)
- 14: $\mathbf{x}_0 = f_V(v_0)$
- 15: $\mathbf{p}'_c = (\mathbf{p}_c + \mathbf{s}_c) / \|\mathbf{p}_c + \mathbf{s}_c\|_2$ for $c \in \mathcal{C}$
- 16: Compute estimate $p(c|\mathbf{x}_0, \mathbf{p}'_c)$ by Eq 2
- 17: **return** $\operatorname{argmax} p$
- 18: **end function**

best to have multiple class-specific representations, each providing complementary information in order to build a holistic representation of that class. Following [30, 38], we can easily improve the robustness of class prototypes by taking the mean of the class-specific embeddings. This allows us to leverage multiple prompting and prompt-learning techniques and retain the knowledge from these various representations. Further, this allows us to maintain the computational and memory efficiency of our method without sacrificing prototype representation strength. We combine the class-agnostic prompts and per-class descriptors to generate the final prototype set $\{\mathbf{p}_c\}_{c \in \mathcal{C}}$. Several types of combinations are discussed in the Appendix.

Prototypes as a plug-and-play module. It is also important to note that our method is not limited to using these aforementioned prompting strategies and, provided that they are embedded within the CLIP text embedding space, is agnostic to how the prototypes are generated. In essence, this makes the prototypes a flexible plug-and-play module of our framework, enabling our framework to take advantage of future advancements in prototype creation.

3.2.3 Test-Time Training and Inference

At test time, given a single test image v_0 , we follow [43] to augment it $(n-1)$ times and compute the features of the original and augmented images with the CLIP image encoder to obtain embeddings $\{\mathbf{x}_i\}_{i=0}^{n-1}$. As introduced in Section 3.2.1, we shift the pre-cached prototypes $\{\mathbf{p}_c\}_{c \in \mathcal{C}}$ to obtain $\{\mathbf{p}'_c\}_{c \in \mathcal{C}}$. For each image

feature \mathbf{x}_i , the predicted probabilities are calculated as

$$p(c|\mathbf{x}_i, \mathbf{p}'_c) = \frac{\exp(\mathbf{p}'_c{}^\top \mathbf{x}_i / \tau)}{\sum_{c \in \mathcal{C}} \exp(\mathbf{p}'_c{}^\top \mathbf{x}_i / \tau)} \quad (2)$$

where τ denotes the temperature scalar. Similar to TPT [43], we select the k distributions with highest confidence (*i.e.* lowest entropy) of the batch and take the average. Denoting the image embeddings corresponding to the selected k distributions as $\{\mathbf{x}'_i\}_{i=1}^k$, we train our model to minimize the following entropy of this marginal distribution,

$$\mathcal{L} = - \sum_{c \in \mathcal{C}} \tilde{p}(c|\mathbf{x}_0, \mathbf{p}'_c) \log \tilde{p}(c|\mathbf{x}_0, \mathbf{p}'_c) \quad (3)$$

$$\text{where } \tilde{p}(c|\mathbf{x}_0) = \frac{1}{k} \sum_{i=1}^k p(c|\mathbf{x}'_i, \mathbf{p}'_c) \quad (4)$$

In our model, the only parameters that are optimized are the shift vectors $\{\mathbf{s}_c\}_{c \in \mathcal{C}}$. We update the shift vectors for a single step of gradient descent.

After test-time training, we encode the original image and compute its cosine similarity with the shifted class prototypes, resulting in a final prediction that is the `argmax` of the prediction logits. Algorithm 1 summarizes the entire procedure of our proposed method, TPS, that enables efficient test-time adaptation using VLMs.

4 Experimental Results

4.1 Datasets

We evaluate our method TPS on natural distributions shifts and cross-dataset generalization. For natural distribution shifts, we evaluate ImageNet [5] along with its four variants: ImageNet-V2 [39], ImageNet-A [15], ImageNet-R [14] and ImageNet-Sketch [50]. For cross-dataset generalization, we evaluate on ten publicly available image classification datasets of different objects and scenes, including fine-grained and specialized datasets: Flowers102 [31], DTD [4], Oxford-Pets [35], StanfordCars [21], UCF101 [45], Caltech101 [6], Food101 [1], SUN397 [51], FGVC-Aircraft [29], and EuroSAT [13]. We report Top-1 accuracy for image classification on all datasets.

4.2 Implementation Details

Similar to TPT [43], we augment a test image 63 times with random resized crops to obtain a batch of 64 images that also includes the original image. We select 10% of samples in the batch with lowest entropy and compute the marginal entropy of the selected predicted probability distributions. We initialize the learnable shift to all zeros and optimize it for 1 step using the AdamW [27] optimizer

Table 1: Acc@1 of zero-shot image classification with CLIP-ViT-B/16 backbone on ImageNet and its OOD variants. Performance improvements over zero-shot CLIP are denoted in (\uparrow blue). Best performances are in **bold**.

Method	ImageNet	ImageNet-A	ImageNet-V2	ImageNet-R	ImageNet-Sketch	Average	OOD Average
	<i>Zero-Shot Baseline</i>						
CLIP-ViT-B/16	66.74	47.79	60.89	73.99	46.12	59.10	57.20
	<i>Test-Time Adaption Baselines</i>						
TPT [43]	68.98	54.77	63.45	77.06	47.94	62.44	60.81
TPT [43] + descriptors*	67.71	54.28	61.24	73.39	46.09	60.54	58.75
TPT + (templates + descriptors)*	69.54	55.13	63.95	77.46	48.34	62.88	61.22
DiffTPT [7]	70.30	55.68	65.10	75.00	46.80	62.28	60.52
Diffusion-TTA [37]	63.8	-	-	-	-	-	-
Ours (Shift + templates + descriptors)	71.45 _(\uparrow4.71)	60.61 _(\uparrow12.82)	64.91 _(\uparrow4.02)	80.20 _(\uparrow6.21)	50.88 _(\uparrow4.76)	65.61 _(\uparrow6.51)	64.15 _(\uparrow6.90)

and learning rate of 5e-3 for ImageNet variants and 1e-3 for cross-dataset generalization. For our method, we initialize each class prototype by taking the micro average of the mean of the class-agnostic CLIP template prompts and the mean of the class-specific GPT-4 generated descriptive prompts.

4.3 Comparison to State-of-the-Art

4.3.1 Baselines We compare our method with zero-shot and TTA baselines that leverage CLIP ViT-B/16 as a backbone. These TTA methods include TPT [43] which performs text-prompt tuning, DiffTPT [7], a variant of TPT that uses diffusion models to augment the visual training data, and Diffusion-TTA [37], a method that adapts a discriminative classifier via a conditional diffusion model. To make our method more comparable to the simplest baselines, we also add their versions using more advanced prototypes, such as the inclusion of class-agnostic CLIP templates [38] (+ **templates**), class-specific LLM-generated descriptors (+ **descriptors**), and learned CoOp [56] prompts (+ **CoOp**).

Given that Test-Time Prompt Tuning (TPT) does not involve tuning in the feature space, our advanced prompt generation is constrained to enhancing the input of TPT’s text encoder. To address this, we append descriptors to the prompt suffixes, denoted as + **descriptors***. Moreover, a limitation arises with TPT’s methodology of initializing its learnable prompt using a singular prompt template. This restricts the potential for integrating the diverse array of CLIP ImageNet prompt templates, as they are structured in various formats. As a result, to further augment the TPT-tuned class prototypes, we take its mean with the same advanced prototypes used at initialization in our method, denoted as +(**templates** + **descriptors**)*.

4.3.2 Natural Distribution Shifts Table 1 presents the top-1 accuracy of our method, benchmarked against zero-shot and test-time adaptation (TTA) baselines using CLIP on ImageNet and its out-of-distribution variants. Our results demonstrate that shifting class prototypes significantly enhances performance. Compared to the baseline zero-shot CLIP, we observe an improvement of 7%, and a 3.3% increase over the vanilla TPT on average for out-of-distribution

Table 2: Acc@1 of zero-shot image classification with CLIP-ViT-B/16 backbone on ImageNet and its OOD variants using CoOp-learned prompts. Performance improvements over zero-shot CLIP are denoted in (\uparrow blue). Best performances are in **bold**.

Method	ImageNet	ImageNet-A	ImageNet-V2	ImageNet-R	ImageNet-Sketch	Average	OOD Average
<i>Zero-Shot Baseline</i>							
CLIP-ViT-B/16 + CoOp [56]	71.51	49.71	64.20	75.21	47.99	61.72	59.28
<i>Test-Time Adaption Baselines</i>							
TPT + CoOp ([43, 56])	73.61	57.95	66.83	77.27	49.29	64.99	62.83
DiffTPT + CoOp ([7, 50])	75.00	58.09	66.80	73.90	49.50	64.12	61.97
Ours (Shift + CoOp [56])	73.73(\uparrow 2.22)	60.49 (\uparrow 10.78)	66.84 (\uparrow 2.64)	77.44 (\uparrow 2.23)	49.08(\uparrow 1.09)	65.52 (\uparrow 3.80)	63.46 (\uparrow 4.18)

Table 3: Acc@1 of zero-shot image classification with CLIP-ViT-B/16 backbone on cross-dataset generalization. Performance improvements over zero-shot CLIP are denoted in (\uparrow blue). Best performances are in **bold**.

Method	Flower102	DTD	Pets	Cars	UCF101	CalTech101	Food101	SUN397	Aircraft	EuroSAT	Average
<i>Zero-Shot Baseline</i>											
CLIP-ViT-B/16	67.28	44.44	87.98	65.24	65.08	92.98	83.80	62.55	23.70	41.42	63.45
<i>Test-Time Adaption Baselines</i>											
TPT [43]	68.98	47.75	87.79	66.87	68.04	94.16	84.67	65.50	24.78	42.44	65.10
TPT [43] + descriptors*	69.14	51.48	86.05	64.84	70.10	93.59	81.83	65.44	22.29	42.98	64.77
TPT + (templates + descriptors)*	69.71	46.93	87.87	66.77	68.60	94.12	84.94	66.11	23.37	43.17	65.16
DiffTPT [7]	70.10	47.00	88.22	67.01	68.22	92.49	87.23	65.74	25.60	43.13	65.47
Diffusion-TTA [37]	71.5	-	86.1	-	-	-	88.8	-	24.6	-	-
Ours (Shift + templates + descriptors)	71.54 (\uparrow 4.20)	50.47(\uparrow 6.09)	87.35(\uparrow 0.63)	69.06 (\uparrow 3.82)	71.00 (\uparrow 5.92)	95.09 (\uparrow 2.11)	85.23(\uparrow 1.43)	68.98 (\uparrow 6.43)	26.34 (\uparrow 2.64)	44.48 (\uparrow 8.06)	66.96 (\uparrow 8.31)

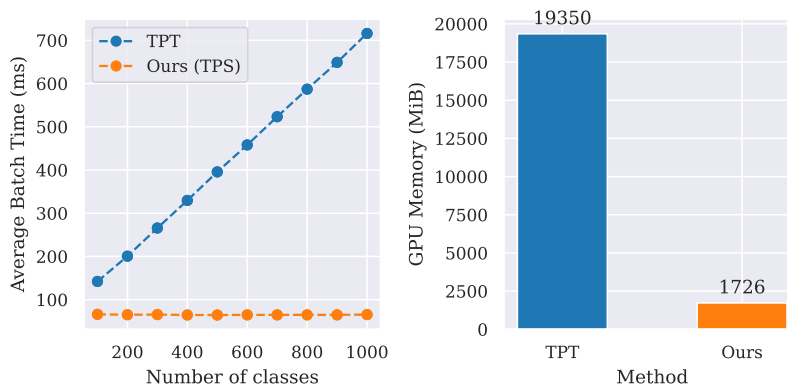
datasets. Furthermore, Table 1 shows that directly appending descriptors to the TPT prompt suffixes results in a performance decrease of 2%, emphasizing the limitations of TPT in seamlessly incorporating prompt-engineering techniques. Notably, Table 2 demonstrates that our approach of learning a feature-based shift outperforms TPT and DiffTPT by 0.6% and 1.5%, respectively, on average even when using advanced prototypes derived from learned CoOp [56] prompts without backpropagating through the text encoder or prompting a diffusion model. This finding underscores that feature space modulation can effectively replicate the impact of test-time prompt tuning in scenarios involving natural distribution shifts.

4.3.3 Cross-Dataset Generalization Table 3 details the performance of our approach relative to zero-shot and test-time adaptation (TTA) baselines when generalizing to fine-grained and specialized datasets. Our findings reveal that the optimal implementation of our method, which involves shifting class prototypes and integrating both CLIP templates and Large Language Model (LLM)-generated descriptors, results in an average improvement of 3.5% over the zero-shot CLIP, and a 1.9% increase compared to TPT.

4.3.4 Comparison to Training-Free Methods In a similar spirit to zero-shot test-time adaptation, training-free methods perform domain adaptation without tuning any parameters. We compare our method to state-of-the-art training-free methods in Table 4. We show that our method, TPS, when using the same GPT-3-generated [2] text prompts from the official SuS-X [47]

Table 4: Acc@1 of zero-shot image classification with CLIP-ResNet-50 backbone on ImageNet and its OOD variants. Best performances are in **bold**.

Method	ImageNet	ImageNet-R	ImageNet-Sketch	Cross-Dataset Average	Needs Support Set
SuS-X-SD-C [47]	61.65	61.69	35.88	60.49	✓
SuS-X-LC-P [47]	61.80	61.62	36.25	60.64	✓
CALIP [11]	60.57	-	-	59.34	✗
Ours (Shift + SuS-X descriptors)	63.52	63.66	37.66	61.47	✗

**Fig. 3:** Comparison of computational and memory costs on an A6000 GPU on ImageNet. Left: Average runtimes of TPT and TPS across different sized subsets of ImageNet [5] over 3 runs. Note that error bars are depicted but are not visible as they have extremely small standard deviations. Right: Memory consumption of TPT and TPS on ImageNet.

code, out-performs both CALIP [11] and SuS-X [47] without any additional image support set constructed with Stable Diffusion [40] or LAION-5B [42]. This demonstrates how a simple feature-space shift is more effective than complex training-free methods. For fair comparison, we compare TPS with SuS-X results with fixed hyperparameter settings as ours are not tuned per dataset and use the same CLIP-ResNet50 backbone.

4.4 Efficiency Analysis

The purpose of test-time adaptation is to tune a model on an out-of-distribution dataset at test-time given a single input or batch at a time. Given that the input is streaming, each adaptation requires low memory and computational cost to be used in practice. TPT [43], by design, tunes the input features to the text encoder. Despite tuning few parameters overall, computing the gradient of the loss with respect to the prompt parameters necessitates the computation of gradients for the parameters in entire text encoder. Computing these gradients

Table 5: Acc@1 for zero-shot image classification comparing pure zero-shot baselines vs. with learned feature-space shift from prototypes derived from various prompts using CLIP-ViT/B-16 backbone.

Prompt Type	Setting	ImageNet	ImageNet OOD Average	Cross-Dataset Average
Vanilla	Zero-Shot	66.74	57.20	63.45
	+ shift	68.77	61.59	64.41
	Δ	+ 2.03	+ 4.39	+ 0.96
CoOp [56]	Zero-Shot	71.51	59.28	N/A
	+ shift	73.73	63.46	N/A
	Δ	+ 2.22	+ 4.18	N/A
CLIP templates	Zero-Shot	68.35	59.43	64.69
	+ shift	70.38	64.04	65.57
	Δ	+ 2.03	+ 4.61	+ 0.88
Descriptors	Zero-Shot	68.52	58.29	66.02
	+ shift	70.40	62.48	66.80
	Δ	+ 1.88	+ 4.19	+ 0.78
CLIP templates + Descriptors	Zero-Shot	69.54	59.88	65.94
	+ shift	71.45	64.15	66.96
	Δ	+ 1.91	+ 4.27	+ 1.02

adds to the runtime, scaling linearly with the number of classes in the dataset, and retaining the encoder gradients adds to the memory requirements.

Figure 3 shows the average batch runtime and GPU memory consumption on ImageNet for TPS and the simplest TTA baseline TPT on a single A6000 GPU. We show the runtime of TPT and TPS on subsets of ImageNet comprised of different sized label sets. We observe that the average runtime per test input for TPT scales linearly with the size of the label set while our method, TPS, remains constant at approximately 65 ms per batch on average. On the full ImageNet test set, we further see that TPS runs **more than 10x as fast** and uses **less than 10x the memory** as TPT, and yet is able to achieve performance gains over the baseline. These significant speed-ups and low memory constraints enable our method to be easily used in practice.

4.5 Ablation Studies

4.5.1 Effect of Shift on Different Prototypes We explore the effect of feature-space shift on a variety of prototypes. Specifically, we compare our method TPS against zero-shot performance given the same prototypes constructed from the vanilla “*a photo of a {class}*” prompt, CoOp [56]-learned prompt, the 80 ImageNet context prompts from CLIP [38] and our LLM-generated descriptors. As observed in Table 5, regardless of the prototype generation technique used, introducing even minor perturbations to class prototypes consistently yields an average gain of $> 4\%$ in top-1 accuracy on ImageNet out-of-distribution datasets and up to 1% on cross-domain datasets over zero-shot CLIP with the same prototypes. This illustrates how the structure of the embedding space is maintained with a learnable shift.

4.5.2 Feature-Space Transformation Variants We compare different variants for feature-space transformations in Table 6. Specifically, we compare against

Table 6: Acc@1 of zero-shot image classification comparing different learned feature transformations using CLIP-ViT-B/16 backbone. Best performances are in **bold**. Second best performances are underlined.

Method	ImageNet	ImageNet OOD Average	Cross-Dataset Average
Scale	70.40	61.12	65.96
Shift	<u>71.45</u>	<u>64.15</u>	66.96
Scale & Shift	71.47	64.16	<u>66.91</u>
FiLM	0.09	0.28	2.08

element-wise *scale*, element-wise *scale&shift*, as well as *FiLM* [36] where affine vectors are computed via a linear layer on the prototypes. We observe that *scale* performs worse than *shift*, and *scale&shift* performs equally to *shift*. On the other hand, *FiLM* suffers from model collapse due to much more learnable weights in TTA. Considering both efficiency and efficacy, *shift* is the best choice in our framework.

5 Conclusion

In this work, we have presented the Test-time Prototype Shifting (TPS) framework, a novel approach to enhancing the zero-shot generalization abilities of VLMs. TPS addresses the limitations of existing test-time training methods, such as Text-Prompt Tuning, by directly modulating class prototypes in the embedding space. This strategy not only reduces the computational and memory demands significantly but also allows for greater flexibility and precision in adapting to diverse domain shifts. By leveraging pre-computed and cached prototypes, and introducing class-specific shifts, TPS effectively bridges domain gaps. The extensive evaluations conducted across multiple datasets demonstrate the superior performance of our method, outperforming existing approaches in terms of accuracy while being more computationally efficient. This work not only sets a new standard for zero-shot generalization in VLMs but also presents a scalable, efficient solution for real-world applications.

6 Research Impact and Limitations

We propose TPS, a framework that can be used to easily and effectively improve zero-shot generalization of VLMs. Given the large-scale training of foundation VLMs, we believe it is important to understand different ways to better leverage the resulting rich multi-modal contrastive representation spaces in parameter- and runtime-constrained settings. We propose to learn a slight perturbation to the class prototypes to maintain the overall representation quality of the pre-trained embedding space while learning a better alignment to the OOD target dataset. We hope that this framework can inspire future work to explore other tasks where learning directly in the feature space can be an efficient alternative to more complex tuning approaches.

Our work builds on the CLIP [38] representation space and uses GPT-4 [34] to generate class descriptors to create more advanced class prototypes. Thus, our model has the potential to magnify the biases of both these models. Future studies may explore how to best leverage these models' capabilities without promoting its biases.

References

1. Bossard, L., Guillaumin, M., Van Gool, L.: Food-101 – mining discriminative components with random forests. In: European Conference on Computer Vision (2014) [9](#)
2. Brown, T.B., Mann, B., Ryder, N., Subbiah, M., Kaplan, J., Dhariwal, P., Neelakantan, A., Shyam, P., Sastry, G., Askell, A., Agarwal, S., Herbert-Voss, A., Krueger, G., Henighan, T., Child, R., Ramesh, A., Ziegler, D.M., Wu, J., Winter, C., Hesse, C., Chen, M., Sigler, E., Litwin, M., Gray, S., Chess, B., Clark, J., Berner, C., McCandlish, S., Radford, A., Sutskever, I., Amodei, D.: Language models are few-shot learners. In: NeurIPS (2020) [4](#), [11](#)
3. Chen, T., Lucic, M., Houlsby, N., Gelly, S.: On self modulation for generative adversarial networks. In: International Conference on Learning Representations (2019) [4](#)
4. Cimpoi, M., Maji, S., Kokkinos, I., Mohamed, S., Vedaldi, A.: Describing textures in the wild. In: Proceedings of the IEEE Conf. on Computer Vision and Pattern Recognition (CVPR) (2014) [9](#)
5. Deng, J., Dong, W., Socher, R., Li, L.J., Li, K., Fei-Fei, L.: ImageNet: A Large-Scale Hierarchical Image Database. In: CVPR (2009) [9](#), [12](#)
6. Fei-Fei, L., Fergus, R., Perona, P.: Learning generative visual models from few training examples: An incremental bayesian approach tested on 101 object categories. In: CVPR Workshops (2004) [9](#)
7. Feng, C.M., Yu, K., Liu, Y., Khan, S., Zuo, W.: Diverse data augmentation with diffusions for effective test-time prompt tuning. In: Proceedings of the IEEE/CVF International Conference on Computer Vision (ICCV). pp. 2704–2714 (October 2023) [3](#), [10](#), [11](#)
8. Gao, P., Geng, S., Zhang, R., Ma, T., Fang, R., Zhang, Y., Li, H., Qiao, Y.: Clip-adapter: Better vision-language models with feature adapters (2021) [2](#)
9. Girdhar, R., El-Nouby, A., Liu, Z., Singh, M., Alwala, K.V., Joulin, A., Misra, I.: Imagebind: One embedding space to bind them all. In: Conference on Computer Vision and Pattern Recognition (CVPR) (2023) [1](#)
10. Goyal, S., Sun, M., Raghunathan, A., Kolter, J.Z.: Test time adaptation via conjugate pseudo-labels. In: Advances in Neural Information Processing Systems. vol. 35, pp. 6204–6218 (2022) [3](#)
11. Guo, Z., Zhang, R., Qiu, L., Ma, X., Miao, X., He, X., Cui, B.: Calip: Zero-shot enhancement of clip with parameter-free attention. In: AAI (2023) [4](#), [12](#)
12. Hassan, J., Gani, H., Hussein, N., Khattak, M.U., Naseer, M., Khan, F.S., Khan, S.: Align your prompts: Test-time prompting with distribution alignment for zero-shot generalization. In: Thirty-seventh Conference on Neural Information Processing Systems (2023) [3](#)
13. Helber, P., Bischke, B., Dengel, A., Borth, D.: Eurosat: A novel dataset and deep learning benchmark for land use and land cover classification. IEEE J. Sel. Top. Appl. Earth Obs. Remote. Sens. (2019) [9](#)
14. Hendrycks, D., Basart, S., Mu, N., Kadavath, S., Wang, F., Dorundo, E., Desai, R., Zhu, T., Parajuli, S., Guo, M., Song, D., Steinhardt, J., Gilmer, J.: The many faces of robustness: A critical analysis of out-of-distribution generalization. ICCV (2021) [9](#)
15. Hendrycks, D., Zhao, K., Basart, S., Steinhardt, J., Song, D.: Natural adversarial examples. In: Proceedings of the IEEE/CVF Conference on Computer Vision and Pattern Recognition (CVPR). pp. 15262–15271 (June 2021) [9](#)

16. Hounsby, N., Giurciu, A., Jastrzebski, S., Morrone, B., De Laroussilhe, Q., Gesmundo, A., Attariyan, M., Gelly, S.: Parameter-efficient transfer learning for NLP. In: Proceedings of the 36th International Conference on Machine Learning (2019) [2](#)
17. Huang, X., Belongie, S.: Arbitrary style transfer in real-time with adaptive instance normalization. In: ICCV (2017) [4](#)
18. Iwasawa, Y., Matsuo, Y.: Test-time classifier adjustment module for model-agnostic domain generalization. In: Advances in Neural Information Processing Systems (2021) [3](#)
19. Jaderberg, M., Simonyan, K., Zisserman, A., kavukcuoglu, k.: Spatial transformer networks. In: Advances in Neural Information Processing Systems. vol. 28 (2015) [4](#)
20. Jia, M., Tang, L., Chen, B.C., Cardie, C., Belongie, S., Hariharan, B., Lim, S.N.: Visual prompt tuning. In: European Conference on Computer Vision (ECCV) (2022) [2](#)
21. Krause, J., Stark, M., Deng, J., Fei-Fei, L.: 3d object representations for fine-grained categorization. In: ICCV Workshops (2013) [9](#)
22. Lester, B., Al-Rfou, R., Constant, N.: The power of scale for parameter-efficient prompt tuning. In: Proceedings of the 2021 Conference on Empirical Methods in Natural Language Processing (Nov 2021) [2](#)
23. Lian, D., Zhou, D., Feng, J., Wang, X.: Scaling & shifting your features: A new baseline for efficient model tuning. In: Advances in Neural Information Processing Systems (NeurIPS) (2022) [4](#)
24. Lin, W., Mirza, M.J., Kozinski, M., Possegger, H., Kuehne, H., Bischof, H.: Video test-time adaptation for action recognition. In: CVPR (2023) [3](#)
25. Liu, S., Yu, S., Lin, Z., Pathak, D., Ramanan, D.: Language models as black-box optimizers for vision-language models (2023) [4](#)
26. Liu, Y., Kothari, P., van Delft, B., Bellot-Gurlet, B., Mordan, T., Alahi, A.: Ttt++: When does self-supervised test-time training fail or thrive? In: Advances in Neural Information Processing Systems. vol. 34, pp. 21808–21820. Curran Associates, Inc. (2021) [3](#)
27. Loshchilov, I., Hutter, F.: Decoupled weight decay regularization. In: International Conference on Learning Representations (2019) [9](#)
28. Ma, X., ZHANG, J., Guo, S., Xu, W.: Swapprompt: Test-time prompt adaptation for vision-language models. In: Thirty-seventh Conference on Neural Information Processing Systems (2023) [3](#)
29. Maji, S., Kannala, J., Rahtu, E., Blaschko, M., Vedaldi, A.: Fine-grained visual classification of aircraft. Tech. rep. (2013) [9](#)
30. Menon, S., Vondrick, C.: Visual classification via description from large language models. ICLR (2023) [2](#), [4](#), [8](#)
31. Nilsback, M.E., Zisserman, A.: Automated flower classification over a large number of classes. In: Indian Conference on Computer Vision, Graphics and Image Processing (Dec 2008) [9](#)
32. Niu, S., Wu, J., Zhang, Y., Chen, Y., Zheng, S., Zhao, P., Tan, M.: Efficient test-time model adaptation without forgetting. In: ICML (2022) [3](#)
33. Niu, S., Wu, J., Zhang, Y., Wen, Z., Chen, Y., Zhao, P., Tan, M.: Towards stable test-time adaptation in dynamic wild world. ICLR (2023) [3](#)
34. OpenAI: Gpt-4 technical report (2023) [7](#), [15](#), [3](#)
35. Parkhi, O.M., Vedaldi, A., Zisserman, A., Jawahar, C.V.: Cats and dogs. In: CVPR (2012) [9](#)

36. Perez, E., Strub, F., de Vries, H., Dumoulin, V., Courville, A.C.: Film: Visual reasoning with a general conditioning layer. In: AAAI (2018) [4](#), [14](#)
37. Prabhudesai, M., Ke, T.W., Li, A.C., Pathak, D., Fragkiadaki, K.: Test-time adaptation of discriminative models via diffusion generative feedback. In: Conference on Neural Information Processing Systems (2023) [4](#), [10](#), [11](#)
38. Radford, A., Kim, J.W., Hallacy, C., Ramesh, A., Goh, G., Agarwal, S., Sastry, G., Askell, A., Mishkin, P., Clark, J., Krueger, G., Sutskever, I.: Learning transferable visual models from natural language supervision. In: ICML (2021) [1](#), [2](#), [3](#), [4](#), [5](#), [7](#), [8](#), [10](#), [13](#), [15](#)
39. Recht, B., Roelofs, R., Schmidt, L., Shankar, V.: Do ImageNet classifiers generalize to ImageNet? In: Proceedings of the 36th International Conference on Machine Learning. Proceedings of Machine Learning Research, vol. 97, pp. 5389–5400. PMLR (09–15 Jun 2019) [9](#)
40. Rombach, R., Blattmann, A., Lorenz, D., Esser, P., Ommer, B.: High-resolution image synthesis with latent diffusion models. In: Proceedings of the IEEE/CVF Conference on Computer Vision and Pattern Recognition (CVPR). pp. 10684–10695 (June 2022) [12](#)
41. Schneider, S., Rusak, E., Eck, L., Bringmann, O., Brendel, W., Bethge, M.: Improving robustness against common corruptions by covariate shift adaptation. In: NeurIPS (2020) [3](#)
42. Schuhmann, C., Beaumont, R., Vencu, R., Gordon, C., Wightman, R., Cherti, M., Coombes, T., Katta, A., Mullis, C., Wortsman, M., Schramowski, P., Kundurthy, S., Crowson, K., Schmidt, L., Kaczmarczyk, R., Jitsev, J.: Laion-5b: An open large-scale dataset for training next generation image-text models. In: Advances in Neural Information Processing Systems. vol. 35, pp. 25278–25294. Curran Associates, Inc. (2022) [12](#)
43. Shu, M., Nie, W., Huang, D.A., Yu, Z., Goldstein, T., Anandkumar, A., Xiao, C.: Test-time prompt tuning for zero-shot generalization in vision-language models. In: Advances in Neural Information Processing Systems. vol. 35, pp. 14274–14289. Curran Associates, Inc. (2022) [2](#), [3](#), [5](#), [6](#), [8](#), [9](#), [10](#), [11](#), [12](#), [1](#)
44. Song, J., Lee, J., Kweon, I.S., Choi, S.: Ecotta: Memory-efficient continual test-time adaptation via self-distilled regularization. In: CVPR (2023) [3](#)
45. Soomro, K., Zamir, A.R., Shah, M.: UCF101: A dataset of 101 human actions classes from videos in the wild. CoRR [abs/1212.0402](#) (2012) [9](#)
46. Sun, Y., Wang, X., Zhuang, L., Miller, J., Hardt, M., Efros, A.A.: Test-time training with self-supervision for generalization under distribution shifts. In: ICML (2020) [3](#)
47. Udandarao, V., Gupta, A., Albanie, S.: Sus-x: Training-free name-only transfer of vision-language models. In: ICCV (2023) [4](#), [11](#), [12](#)
48. de Vries, H., Strub, F., Mary, J., Larochelle, H., Pietquin, O., Courville, A.C.: Modulating early visual processing by language. In: Advances in Neural Information Processing Systems. vol. 30 (2017) [4](#)
49. Wang, D., Shelhamer, E., Liu, S., Olshausen, B.A., Darrell, T.: Tent: Fully test-time adaptation by entropy minimization. In: ICLR (2021) [3](#)
50. Wang, H., Ge, S., Lipton, Z., Xing, E.P.: Learning robust global representations by penalizing local predictive power. In: Advances in Neural Information Processing Systems. pp. 10506–10518 (2019) [9](#)
51. Xiao, J., Hays, J., Ehinger, K.A., Oliva, A., Torralba, A.: Sun database: Large-scale scene recognition from abbey to zoo. In: 2010 IEEE Computer Society Conference on Computer Vision and Pattern Recognition (June 2010). <https://doi.org/10.1109/CVPR.2010.5539970> [9](#)

52. Yang, Y., Panagopoulou, A., Zhou, S., Jin, D., Callison-Burch, C., Yatskar, M.: Language in a bottle: Language model guided concept bottlenecks for interpretable image classification. In: CVPR (2023) [2](#), [4](#)
53. Zhang, M., Levine, S., Finn, C.: MEMO: test time robustness via adaptation and augmentation. CoRR [abs/2110.09506](#) (2021) [3](#)
54. Zhang, M., Levine, S., Finn, C.: Memo: Test time robustness via adaptation and augmentation. In: Advances in Neural Information Processing Systems. vol. 35, pp. 38629–38642. Curran Associates, Inc. (2022) [5](#)
55. Zhao, S., Wang, X., Zhu, L., Yang, Y.: Test-time adaptation with clip reward for zero-shot generalization in vision-language models. In: ICLR (2024) [3](#)
56. Zhou, K., Yang, J., Loy, C.C., Liu, Z.: Learning to prompt for vision-language models. CoRR [abs/2109.01134](#) (2021) [2](#), [4](#), [7](#), [10](#), [11](#), [13](#)
57. Zhou, K., Yang, J., Loy, C.C., Liu, Z.: Conditional prompt learning for vision-language models. In: CVPR (2022) [2](#), [4](#), [7](#)
58. Zhou, Y., Ren, J., Li, F., Zabih, R., Lim, S.N.: Test-time distribution normalization for contrastively learned visual-language models. In: Thirty-seventh Conference on Neural Information Processing Systems (2023) [4](#)

Just Shift It: Test-Time Prototype Shifting for Zero-Shot Generalization with Vision-Language Models Supplementary Material

Elaine Sui, Xiaohan Wang, and Serena Yeung-Levy

Stanford University
{esui, xhanwang, syeung}@stanford.edu

This document provides more details of our approach and additional experimental results, organized as follows:

- § [A](#) Implementation Details.
- § [B](#) Additional Quantitative Results with Different Random Seeds.
- § [C](#) Additional Ablation Studies.

A Implementation Details of TPS

Algorithm 2 shows more detailed pseudocode in PyTorch-like style for Test-Time Prototype Shifting over an entire dataset. We will release the models and source code to ensure reproducibility.

B Main Results With More Random Seeds

In Sec [B.1](#) and [B.2](#), we run Test-Time Prototype Shifting (TPS) over 3 random seeds on both the natural distribution shifts (Table 1) and cross-dataset generalization (Table 3), respectively. The randomness comes from the image augmentation in creating a diverse minibatch for the entropy minimization objective.

B.1 Natural Distribution Shifts

From Table 7, we observe that our conclusion from Sec 4.3.2 still holds. That is, our method outperforms SoTA TPT [43] by $> 3.4\%$ on average. We also observe that augmenting the TPT-tuned class prototypes with more advanced off-the-shelf prototypes only boosts performance by a mere 0.5% on average over vanilla TPT, demonstrating TPT’s limitation in maximally leveraging these advanced prototypes.

B.2 Cross-Dataset Generalization

From Table 8, we see that our conclusion from Sec 4.3.3 remains valid. Specifically, TPS outperforms TPT [43] by $> 2\%$ on average. Similarly to Sec [B.1](#), we observe that taking the mean of the TPT-tuned and advanced off-the-shelf prototypes increases performance by only 0.5% on average over TPT, demonstrating TPT’s inflexibility in utilizing these more robust class representations.

Algorithm 2 Test-Time Prototype Shifting Pseudocode in PyTorch-like style

```

1 # Define frozen parameters
2 image_encoder = CLIPImageEncoder()
3 prototypes = load_class_prototypes()
4
5 predictions = []
6 for img, label in data_loader:
7     # Test-Time Shifting
8     shift_params = nn.Parameter(torch.zeros(num_classes, embed_dim),
9                                 requires_grad=True)
9     aug_imgs = [aug(img) for i in range(batch_size - 1)]
10    imgs = torch.stack([img] + aug_imgs, dim=0)
11    image_features = image_encoder(imgs)
12
13    text_features = prototypes + shift_params
14    text_features = F.normalize(text_features, dim=-1)
15
16    logits = (logit_scale * text_features @ image_features.T)
17
18    # Confidence selection
19    entropies = compute_batch_entropies(logits)
20    top_k_idx = torch.argsort(batch_entropy, descending=False)[:k]
21
22    loss = compute_average_entropy(logits[top_k_idx])
23    optimizer.zero_grad()
24    loss.backward()
25    optimizer.step()
26
27    # Test-Time Inference
28    new_prototypes = prototypes + shift_params
29    new_prototypes = F.normalize(new_prototypes, dim=-1)
30
31    logits = (logit_scale * new_prototypes @ image_features[0].unsqueeze
32              (0).T)
32    pred = torch.argmax(logits)
33
34    predictions.append(pred)
35
36 return predictions

```

Table 7: Acc@1 of zero-shot image classification with CLIP-ViT-B/16 backbone on ImageNet and its OOD variants over 3 random seeds. Best performances are in **bold**.

Method	ImageNet	ImageNet-A	ImageNet-V2	ImageNet-R	ImageNet-Sketch	Average	OOD Average
	<i>Test-Time Adaptation Baselines</i>						
TPT [43]	68.96 (± 0.3)	54.47 (± 2.6)	63.46 (± 0.7)	77.10 (± 0.4)	47.93 (± 0.3)	62.38 (± 0.5)	60.74 (± 0.6)
TPT + (templates + descriptors)*	69.51 (± 0.5)	54.94 (± 1.7)	63.86 (± 1.1)	77.57 (± 1.1)	48.38 (± 0.4)	62.85 (± 0.3)	61.19 (± 0.4)
Ours	71.43 (± 0.6)	60.78 (± 2.1)	65.00 (± 0.9)	80.06 (± 1.3)	50.97 (± 0.9)	65.65 (± 0.6)	64.20 (± 0.8)

Table 8: Acc@1 of zero-shot image classification with CLIP-ViT-B/16 backbone on cross-dataset generalization over 3 random seeds. Best performances are in **bold**.

Method	Flower102	DTD	Pets	Cars	UCF101	CalTech101	Food101	SUN397	Aircraft	EuroSAT	Average
TPT [43]	68.79 (± 1)	46.79 (± 1)	87.09 (± 1)	66.38 (± 2)	67.86 (± 1)	94.13 (± 1)	84.67 (± 1)	65.41 (± 1)	23.44 (± 3)	42.78 (± 3)	64.73 (± 1)
TPT + (templates + descriptors)*	69.67 (± 1.1)	47.56 (± 5.5)	87.88 (± 0.2)	66.91 (± 1.7)	68.35 (± 2.1)	94.17 (± 1.3)	84.89 (± 0.7)	66.23 (± 1.2)	23.55 (± 3.1)	43.12 (± 1.8)	65.23 (± 0.6)
Ours	71.47 (± 1.2)	51.00 (± 4.7)	87.45 (± 0.9)	68.99 (± 1.0)	70.98 (± 2.4)	94.90 (± 1.6)	85.15 (± 0.8)	68.85 (± 1.6)	25.82 (± 4.5)	44.61 (± 1.1)	66.92 (± 0.4)

C Full Ablations

In Sec C.1, we report full ablations on TPS on the effectiveness of feature-space shift on various prototypes. These results are comparable to those reported in Sec 4.5. In Sec C.2, we include additional ablations to observe the effect of learning a class-specific shift over a universal shift for all classes. In Sec C.3, we explore variants on prototype generation using the class-agnostic CLIP ImageNet context prompt templates [38] and the class-specific descriptors generated using GPT-4 [34]. All these ablations are run over 3 random seeds.

C.1 Effect of Shift on Different Prototypes

Full comparisons between zero-shot and feature-shifted performance on all natural distribution shift and cross-domain generalization benchmark datasets over 3 random seeds are in Tables 9 and 10, respectively. We demonstrate that our conclusion from Sec 4.5.1 stills holds – that learning a small perturbation in the feature space results in performance gains of $> 4\%$ and up to 1% on average across natural distribution shift and cross-domain generalization tasks regardless of what prototypes are used.

C.2 Effect of Per-Class vs. Shared Shift

Test-time prompt tuning methods involve tuning a prompt that is shared across all classes in a dataset. Given that the tuneable prompt tokens form a portion of the text encoder input, these full prompts are then mapped to the embedding space with the encoder’s learned complex feature-space mapping. This results in non-linear perturbations from the original class prototypes. However, for our method, tuning shift parameters that are shared for all class prototypes in the feature-space means that the relative distance between class prototypes will remain constant before and after test-time shift tuning, limiting the expressive capability of the learned shift. Rather, we believe that each class prototype should

Table 9: Acc@1 for zero-shot and with feature-space shift with features initialized using different prototype generation techniques on ImageNet and its out-of-distribution variants. Results are over 3 random seeds.

Prompt Type	Setting	ImageNet	ImageNet-A	ImageNet-V2	ImageNet-R	ImageNet-Sketch	Average	OOD Average
Vanilla	Zero-Shot	66.74	47.79	60.89	73.99	46.12	59.10	57.20
	+ shift	68.81 (± 0.03)	58.11 (± 0.16)	63.51 (± 0.17)	76.98 (± 0.05)	48.11 (± 0.09)	63.10 (± 0.08)	61.68 (± 0.09)
	Δ	+ 2.07	+ 10.32	+ 2.62	+ 2.99	+ 1.99	+ 4.00	+ 4.48
CoOp [56]	Zero-Shot	71.51	49.71	64.20	75.21	47.99	61.72	59.28
	+ shift	73.76 (± 0.04)	60.43 (± 0.12)	66.84 (± 0.10)	77.39 (± 0.05)	49.08 (± 0.06)	65.50 (± 0.02)	63.44 (± 0.03)
	Δ	+ 2.25	+ 10.72	+ 2.64	+ 2.18	+ 1.09	+ 3.78	+ 4.16
CLIP templates	Zero-Shot	68.35	49.95	61.97	77.59	48.21	61.21	59.43
	+ shift	70.39 (± 0.06)	60.47 (± 0.07)	64.66 (± 0.04)	80.70 (± 0.04)	50.38 (± 0.14)	65.32 (± 0.03)	64.05 (± 0.02)
	Δ	+ 2.04	+ 10.52	+ 2.69	+ 3.11	+ 2.17	+ 4.11	+ 4.62
Descriptors	Zero-Shot	68.52	48.91	61.78	74.81	47.68	60.34	58.29
	+ shift	70.38 (± 0.03)	59.21 (± 0.09)	63.80 (± 0.07)	77.49 (± 0.12)	49.57 (± 0.06)	64.09 (± 0.02)	62.52 (± 0.03)
	Δ	+ 1.86	+ 10.30	+ 2.02	+ 2.68	+ 1.89	+ 3.75	+ 4.23
CLIP templates + Descriptors	Zero-Shot	69.54	50.51	63.01	77.18	48.84	61.82	59.88
	+ shift	71.43 (± 0.06)	60.78 (± 0.21)	65.00 (± 0.09)	80.06 (± 0.13)	50.97 (± 0.09)	65.65 (± 0.06)	64.20 (± 0.08)
	Δ	+ 1.89	+ 10.27	+ 1.99	+ 2.88	+ 2.13	+ 3.83	+ 4.32

Table 10: Acc@1 for zero-shot and with feature-space shift with features initialized using different prototype generation techniques on cross-domain generalization datasets. Results are over 3 random seeds.

Prompt Type	Setting	Flower102	DTD	Pets	Cars	UCF101	CalTech101	Food101	SUN397	Aircraft	EuroSAT	Average
Vanilla	Zero-Shot	67.28	44.44	87.98	65.24	65.08	92.98	83.80	62.55	23.70	41.42	63.45
	+ shift	67.75 (± 0.10)	45.69 (± 0.10)	87.57 (± 0.10)	67.60 (± 0.23)	66.79 (± 0.21)	93.79 (± 0.08)	84.62 (± 0.03)	64.58 (± 0.03)	24.75 (± 0.39)	41.35 (± 0.03)	64.45 (± 0.04)
	Δ	+ 0.47	+ 1.25	- 0.41	+ 2.36	+ 1.71	+ 0.81	+ 0.82	+ 2.03	+ 1.05	- 0.07	+ 1.00
CLIP templates	Zero-Shot	65.57	44.86	88.25	66.19	67.46	93.67	83.77	65.78	23.64	47.74	64.69
	+ shift	66.41 (± 0.05)	45.61 (± 0.19)	87.99 (± 0.10)	68.66 (± 0.31)	68.02 (± 0.11)	93.85 (± 0.14)	84.54 (± 0.08)	67.19 (± 0.05)	24.66 (± 0.13)	48.28 (± 0.20)	65.52 (± 0.05)
	Δ	+ 0.84	+ 0.75	- 0.26	+ 2.47	+ 0.56	+ 0.18	+ 0.77	+ 1.41	+ 1.02	+ 0.54	+ 0.83
Descriptors	Zero-Shot	71.13	52.72	86.75	65.15	70.53	94.08	84.12	67.10	25.26	43.31	66.02
	+ shift	71.69 (± 0.15)	53.80 (± 0.21)	87.82 (± 0.19)	67.00 (± 0.14)	71.18 (± 0.15)	94.56 (± 0.08)	84.78 (± 0.05)	68.25 (± 0.18)	26.27 (± 0.09)	42.11 (± 0.18)	66.75 (± 0.06)
	Δ	+ 0.56	+ 1.08	+ 1.07	+ 1.85	+ 0.65	+ 0.48	+ 0.66	+ 1.15	+ 1.01	- 1.20	+ 0.73
CLIP templates + Descriptors	Zero-Shot	70.52	49.94	87.22	66.48	70.24	94.12	84.47	67.55	24.69	44.14	65.94
	+ shift	71.47 (± 0.12)	51.00 (± 0.47)	87.45 (± 0.09)	68.99 (± 0.10)	70.98 (± 0.24)	94.90 (± 0.16)	85.15 (± 0.08)	68.85 (± 0.16)	25.82 (± 0.45)	44.61 (± 0.11)	66.92 (± 0.04)
	Δ	+ 0.95	+ 1.06	+ 0.23	+ 2.51	+ 0.74	+ 0.78	+ 0.68	+ 1.30	+ 1.13	+ 0.47	+ 0.98

be modulated by slightly different magnitudes and/or directions to provide more degrees of freedom in capturing the class-level distribution shifts in addition to the dataset-level shifts present in a domain gap.

Table 11 shows that, on average, learning a per-class shift increases performance by $> 1.2\%$ regardless of which prototypes are used. Moreover, we see that Table 12 demonstrates that, on average, learning a per-class shift increases performance by around 0.5% on average over different prototype settings. This demonstrates that learning per-class shifts allows the model to capture both dataset-level and class-level distribution shifts in a domain gap.

C.3 Prototype Variants

We explore different methods for creating class prototypes. Specifically, we experiment with different forms of aggregating the text encoded with the 80 ImageNet context prompts from CLIP [38] and our LLM-generated descriptors. The CLIP ImageNet templates are class-agnostic and add image-level charac-

Table 11: Acc@1 for learning a shared vs. per-class shift on top of different prototypes over 3 random seeds. Best performances are in **bold**.

Method	ImageNet	ImageNet-A	ImageNet-V2	ImageNet-R	ImageNet-Sketch	Average	OOD Average
Shared	71.23 (± 0.02)	56.57 (± 0.19)	64.98 (± 0.03)	79.31 (± 0.03)	50.80 (± 0.06)	64.58 (± 0.04)	62.92 (± 0.06)
Per class	71.43 (± 0.06)	60.78 (± 0.21)	65.00 (± 0.09)	80.06 (± 0.13)	50.97 (± 0.09)	65.65 (± 0.06)	64.20 (± 0.08)

Table 12: Acc@1 for learning a shared vs. per-class shift on top of different prototypes over 3 random seeds. Best performances are in **bold**.

Method	Flower102	DTD	Pets	Cars	UCF101	CalTech101	Food101	SUN397	Aircraft	EuroSAT	Average
Shared	71.36 (± 0.12)	50.49 (± 0.12)	87.46 (± 0.12)	67.33 (± 0.06)	70.77 (± 0.12)	94.35 (± 0.06)	84.82 (± 0.01)	68.12 (± 0.04)	25.27 (± 0.02)	44.67 (± 0.06)	66.47 (± 0.03)
Per-class	71.47 (± 0.12)	51.00 (± 0.47)	87.45 (± 0.09)	68.99 (± 0.10)	70.98 (± 0.24)	94.90 (± 0.16)	85.15 (± 0.08)	68.85 (± 0.16)	25.82 (± 0.45)	44.61 (± 0.11)	66.92 (± 0.04)

teristics whereas the descriptors are class-specific and add class-level semantic information.

Tables 13 and 14 compare three variants of pooling these CLIP templated embeddings and descriptor embeddings to obtain a single class prototype. Similarly to the conclusion of Sec 4.5.1, we observe that in general, the gains observed using more advanced prototypes in the zero-shot setting almost directly translate to the test-time adaptation setting with shifting. In Sec 4, we present the results of our method using prototypes that are a micro average of the CLIP templates and LLM-generated descriptors.

Table 13: Acc@1 for different variants of prototype generation, i.e. ways of combining templates and descriptors, on natural distribution shifts, over 3 random seeds. Best performances for each setting are in **bold**.

Prompt Type(s)	Pooling Method	ImageNet	ImageNet-A	ImageNet-V2	ImageNet-R	ImageNet-Sketch	Average	OOD Average	
Vanilla prompt	N/A	66.74	47.79	60.89	<i>Zero-Shot</i> 73.99		59.10	57.20	
CLIP templates + Descriptors	Macro	68.73	50.32	62.31	77.67	48.56	61.52	59.72	
CLIP templates + Descriptors	Micro	69.54	50.51	63.01	77.18	48.84	61.82	59.88	
CLIP templates × Descriptors	Macro	69.03	50.73	62.22	76.91	49.07	61.59	59.73	
Vanilla prompt	N/A	68.81 (±.03)	58.11 (±.16)	63.51 (±.17)	<i>With Shift</i> 76.98 (±.05)		48.11 (±.09)	63.10 (±.08)	61.68 (±.09)
CLIP templates + Descriptors	Macro	70.75 (±.08)	60.86 (±.09)	64.95 (±.11)	80.84 (±.03)	50.70 (±.11)	65.62 (±.02)	64.34 (±.02)	
CLIP templates + Descriptors	Micro	71.43 (±.06)	60.78 (±.21)	65.00 (±.09)	80.06 (±.13)	50.97 (±.09)	65.65 (±.06)	64.20 (±.08)	
CLIP templates × Descriptors	Macro	70.82 (±.02)	60.42 (±.06)	64.50 (±.05)	79.53 (±.09)	51.13 (±.02)	65.28 (±.01)	63.89 (±.02)	

Table 14: Acc@1 for different variants of knowledge injection, i.e. ways of combining templates and descriptors, over 3 random seeds on cross-dataset generalization tasks. Best performances in each setting are in **bold**.

Prompt Type(s)	Pooling Method	Flower102	DTD	Pets	Cars	UCF101	CaTech101	Food101	SUN397	Aircraft	EuroSAT	Average	
Vanilla prompt	N/A	67.38	44.44	87.98	65.24	65.08	<i>Zero-Shot</i> 92.98		83.80	62.55	23.70	41.42	63.45
CLIP templates + Descriptors	Macro	66.91	45.86	88.33	66.46	68.12	93.83	83.97	66.34	24.03	46.62	65.05	
CLIP templates + Descriptors	Micro	70.52	49.94	87.22	66.48	70.24	94.12	84.47	67.55	24.69	44.14	65.94	
CLIP templates × Descriptors	Macro	72.03	50.83	86.21	66.12	70.90	94.16	83.73	67.98	25.53	47.19	66.47	
Vanilla prompt	N/A	67.75 (±.10)	45.69 (±.10)	87.57 (±.10)	67.69 (±.23)	66.79 (±.21)	<i>With Shift</i> 93.79 (±.08)		84.62 (±.03)	64.58 (±.03)	24.75 (±.39)	41.35 (±.03)	64.45 (±.04)
CLIP templates + Descriptors	Macro	67.52 (±.27)	46.43 (±.28)	88.00 (±.13)	69.04 (±.16)	68.67 (±.18)	94.16 (±.18)	84.77 (±.04)	67.70 (±.08)	24.79 (±.30)	47.09 (±.19)	65.82 (±.06)	
CLIP templates + Descriptors	Micro	71.47 (±.12)	51.00 (±.47)	87.45 (±.09)	68.99 (±.10)	70.98 (±.24)	94.90 (±.16)	85.15 (±.08)	68.85 (±.16)	25.82 (±.45)	44.61 (±.11)	66.92 (±.04)	
CLIP templates × Descriptors	Macro	72.53 (±.12)	52.56 (±.09)	86.15 (±.05)	68.89 (±.07)	71.44 (±.20)	94.43 (±.06)	84.44 (±.08)	69.04 (±.02)	26.51 (±.26)	45.65 (±.15)	67.16 (±.03)	